Cold-Climate Modification of Martian Landscapes: A Case Study of a Spatulate Debris Landform in the Hellas Montes Region, Mars

Abstract

We use spaceborne image and topographic data of Mars for a geomorphological study of the origin, development, and post-emplacement modification of a 30 km-long spatulate landform in the Hellas Montes area, east of Hellas Planitia. The area is characterized by an abundance of lobate debris aprons, all of which have been interpreted as a result of creep and viscous deformation of rock and ice mixtures that make the eastern Hellas Planitia assemblages a type location for possible Martian rock glaciers.

The spatulate landform has been discussed controversially in the past. Explanations range from a rock glacier to a wet debris avalanche or debris flow origin. This work scrutinizes arguments provided in earlier works and presents evidence that a landslide origin of the spatulate landform, connected with a sector collapse of a volcanic construct, is conceivable. We also find extensive observational evidence that the landslide has recently undergone or is still undergoing significant post-emplacement modifications, which are characteristic of rock glaciers in periglacial environments. Creep deformation as well as disintegration of the original surface by thermokarstic degradation are considered to have obliterated impact craters and, in consequence, create a seemingly younger age. Similar processes are considered to be common on Mars under current climatic conditions. Our results imply that the strong and possible long-term modification of landforms on Mars by cold-climate processes often hinders the identification of their original nature and complicates the assessment of true ages.

9.1. Introduction

Lobate debris aprons and valley fill of the fretted terrain at the Martian dichotomy boundary and the southern impact crater structures are considered to be the most pronounced landforms on Mars that are associated with creep or flow of debris containing considerable amounts of ice and water (*Squyres*, 1978; *Lucchitta*, 1984; *Squyres and Carr*, 1986; *Carr*, 1996, 2001).

These features occur in mid-latitudes of both hemispheres and are well developed at the eastern boundary of the Hellas Planitia impact basin (e.g., *Squyres*, 1978, 1979; *Squyres and Carr*, 1986; *Crown et al.*, 1992; *Stewart and Crown*, 1997).

The Hellas/Centauri Montes as well as the large geomorphologic context of the Eastern Hellas Planitia assemblages are one of those areas on Mars that have been discussed by many workers in a wide field of geologic and geomorphologic topics. Landforms and geology of that area are primarily related to the Hellas Planitia impact event which occurred early in
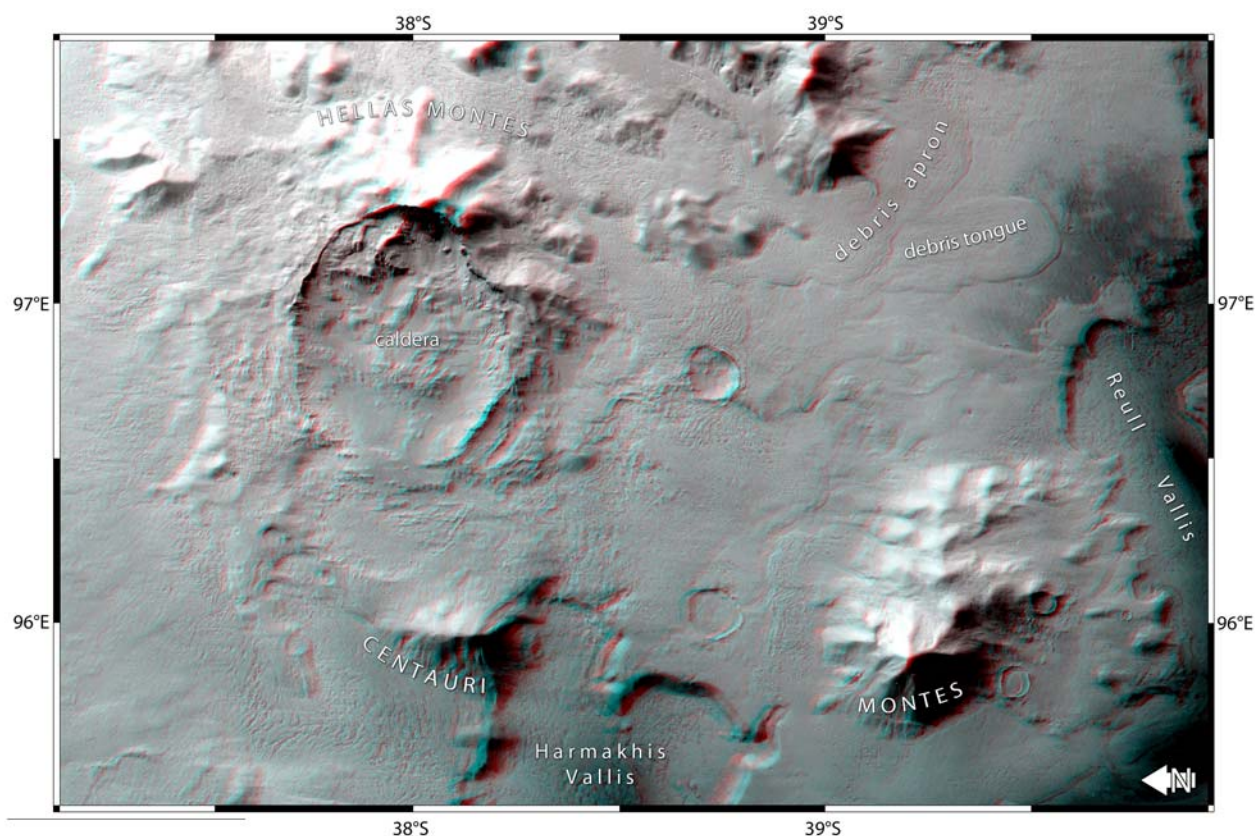
Figure 9.1.: [a] Anaglyph image of the Centauri and western Hellas Montes assemblages showing the debris tongue in context with adjacent debris aprons and other landforms discussed in the main text. Anaglyph is red (left eye), cyan (right eye) and composed of the nadir and stereo-1 channels of a HRSC scene of orbit 2510, stereo angle is 18.9°; north is to the left for correct stereo impression; north is to the left.

Martian history and formed one of the largest impact basins in the solar system (e.g., *Greeley and Guest*, 1987; *Tanaka et al.*, 1992). Subsequently, volcanic processes and resurfacing of landforms connected to Hesperia Planum and the Hadriaca and Tyrrhena Paterae volcanic edifices shaped the area (e.g., *Greeley and Crown*, 1990; *Crown and Greeley*, 1993). Outflow activity connected to the Dao and Niger Valles as well as Harmakhis Vallis (*Price*, 1992; *Bleamaster and Crown*, 2004) and the contributory Reull Vallis caused ongoing resurfacing and mass transport of large amounts of debris (*Leth and Treiman*, 1997; *Mest and Crown*, 2001; *Kostama et al.*, 2006).

Among debris-related lobate landforms in the Eastern Hellas Centauri and Hellas Montes assemblages, a small region centered at 98°E and 37°S shows a prominent spatulate landform which is morphologically different from adjacent lobate features that are commonly compared to terrestrial rock glacier analogues (e.g., *Squyres*, 1978, 1979; *Lucchitta*, 1984; *Crown et al.*, 1992; *Whalley and Azizi*, 2003).

Based upon Viking observations as well as Mars Global Surveyor's Mars Orbiter Camera (MOC) imagery and topographic information from the Mars Orbiter Laser Altimeter (MOLA) combined with Viking stereo data, the elongated landform has been recently interpreted as a wet debris avalanche (*Baratoux et al.*, 2002). This view contrasts to earlier Viking- and MOC-based interpretation of the morphologic inventory in which this landforms is classified as more akin to rock glaciers (*Crown et al.*, 1992). A rock glacier origin was later also supported by ob-
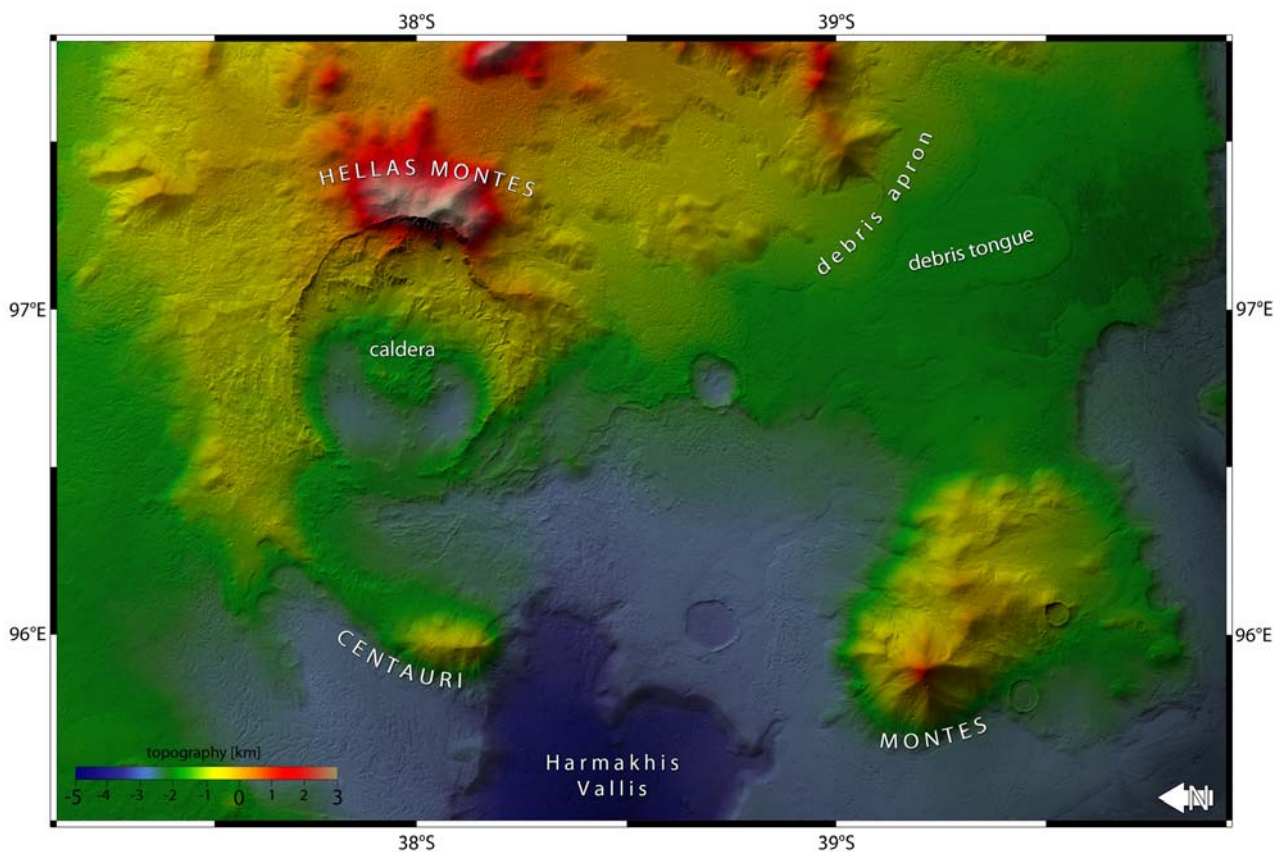
Figure 9.2.: [b] Color-coded MOLA-based topography superimposed on HRSC nadir scene of orbit 2510 covering the Centauri and western Hellas Montes assemblages and showing the debris tongue in context with adjacent debris aprons and other landforms discussed in the main text; heights are above MOLA-defined sphere; north is to the left.

servations by *Degenhardt and Giardino* (2003) as well as *Pierce and Crown* (2003). This landform was also briefly reviewed in *Kargel* (2004, p. 279).

Upon image data provided by the MGS-MOC instrument (*Malin et al.*, 1992) as well as the Mars Odyssey Thermal Emission and Imaging Spectrometer (MO-THEMIS) (*Christensen et al.*, 2004) and the High-Resolution Stereo Camera on Mars Express (MEX-HRSC) (*Neukum et al.*, 2004) details of that landform are studied in more detail herein to allow us to re-assess emplacement conditions and detect possible genetic connections to landforms in adjacent terrain. Data from MGS-MOC, MO-THEMIS and MEX-HRSC were used for image interpretation.

As complimentary mapping source, stereo anaglyphs derived from the stereo channels of MEX-HRSC have been used for the extraction of information on relief, superposition of individual units and context mapping. For morphometric analyses of the debris-tongue landform, topographic profiles (PEDR datasets) derived from MGS-MOLA (*Zuber et al.*, 1992) have been utilized.

9.2. Background

Most recent and most focused work on the formation of the spatulate landform (figure 9.1 and 9.3) states that it formed in the geologically recent past during the late Amazonian as estimated through crater counts and was emplacement as debris flow or wet debris avalanche (*Baratoux et al.*, 2002). In that work, the exact process involved in formation as well as the location of the source area remain relatively uncertain although it is hypothesized that the source area may
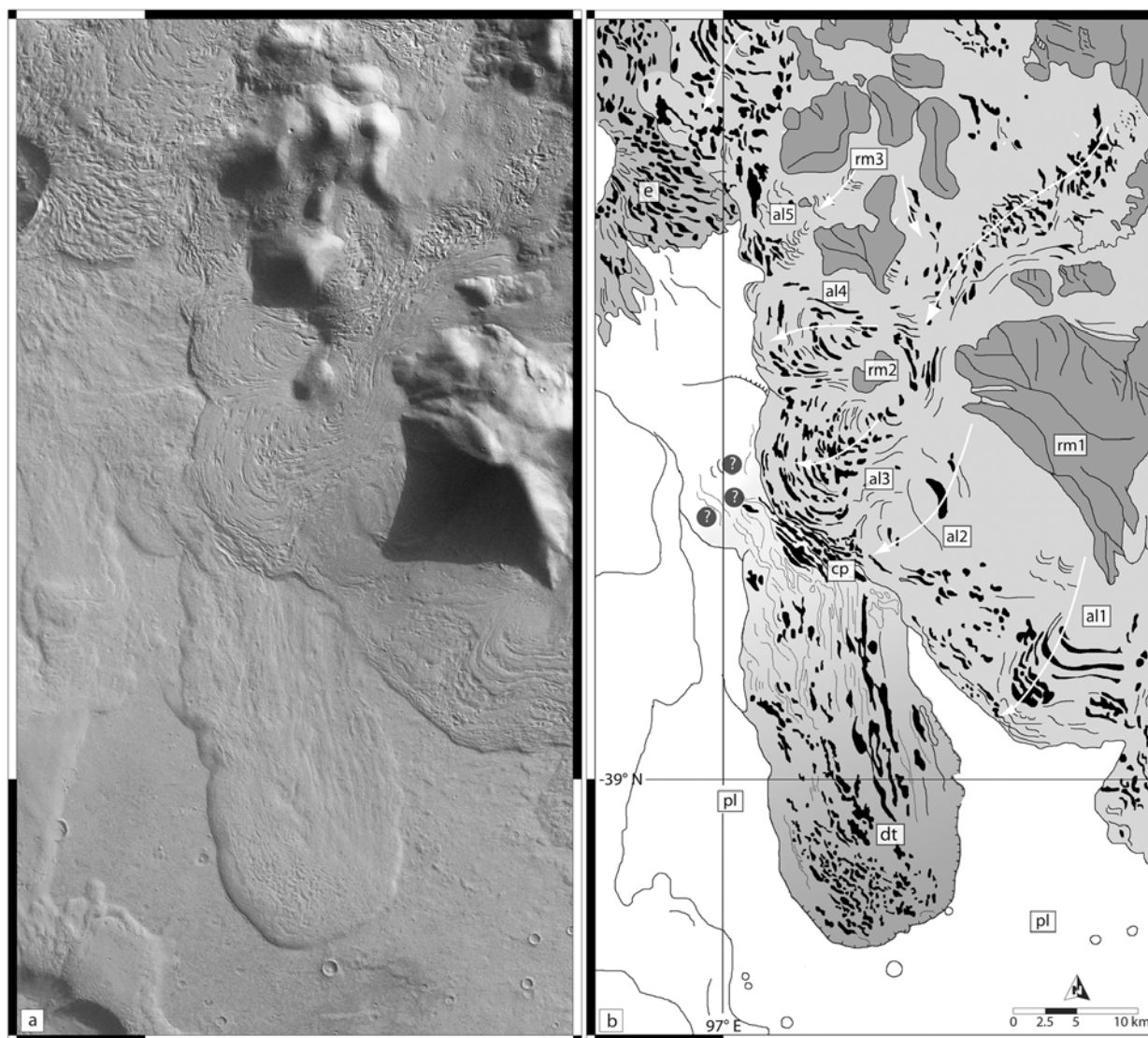
Figure 9.3.: [a] MEX-HRSC nadir scene from orbit 0506 showing spatulate debris tongue (dt) and adjacent area. Note complex and coalescing debris apron lobes (al1-5) emerging from remnant massifs (rm1-4). Remnant massif (rm3) was proposed as possible source area of debris tongue (dt) by (*Baratoux et al.*, 2002), see also figure 9.9, illumination is from top right; [b] Sketch map indicating patterns characteristic of flow consisting of compressional and extensional features.

be located near a small complex of remnant knobs north of the debris tongue (figure 9.1 and rm3 in figure 9.3, figure 9.9) (*Baratoux et al.*, 2002).

Based on estimates of the net resistance coefficient *R*, a descriptive parameter of the conversion of gravitational energy to an unrecoverable form during debris flow motion, which can be determined through the height-to-length ratio (*H/L*) of the tongue-shaped landform (*Iverson et al.*, 1997), *Baratoux et al.* (2002) compared morphometric data to terrestrial debris

flows, glacial-outburst floods and other water- or ice-debris transport systems (*Scheidegger* (1973); *Campbell* (1989); *Iverson et al.* (1997) as cited in *Baratoux et al.* (2002)).

For the Martian spatulate feature, *R* was estimated to be in the range of $R = 25 - 65$ with H= 800 ± 250 m and L= 30 ± 5 km. The exact values for the length and height of the debris tongue remain unknown as the location of the source area is uncertain and no information on the subsurface relief can be obtained. The
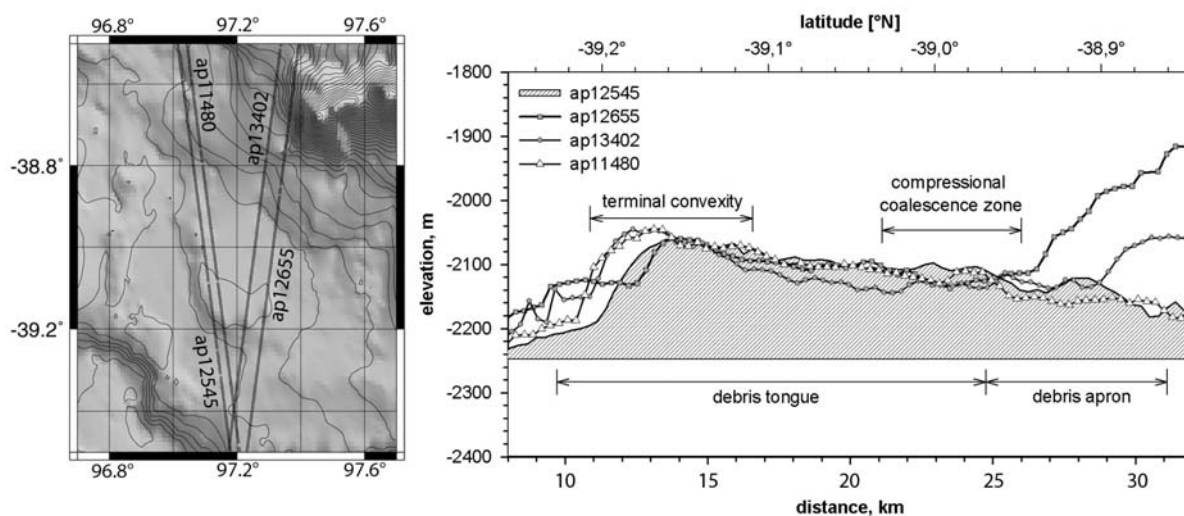
Figure 9.4.: Laser-altimetry based shaded relief map and topographic profiles of the debris tongue and adjacent areas based on MOLA PEDR final datasets. Note typical convex shape of debris tongue terminus comparable to lobate debris aprons at coalescence zone.

interpretation by *Baratoux et al.* (2002) was furthermore supported by the shape of this landform's longitudinal profile as it does not show a typical convex-upward shape indicative of viscous deformation of ice and debris as frequently observed at terminal surfaces of lobate debris aprons (*Squyres*, 1978; *Mangold*, 2001).

Instead, the proposed concave-upward profile would suggest rapid debris transport through water-rich flow and accumulation of a dam at the flow terminus as frequently observed at termini of terrestrial avalanches (*Iverson*, 1997; *Iverson et al.*, 1997). Further features such as missing compressional ridges on the flow surface and the general well-confined appearance at the flow margins were also interpreted as characteristics for debris avalanches.

The arguments as summarized above led *Baratoux et al.* (2002) to the conclusion that the landform is most probably a wet debris avalanche that is derived from an uncertain location. Its proposed young age contradicts the stability of liquid water in the recent past in the subsurface and therefore, considerable amounts of water must have been released to facilitate emplacement of the debris tongue that was initiated by a process unknown yet (*Baratoux et al.*, 2002).

9.3. Debris-Tongue Characteristics

9.3.1. General Settings and Shape

The spatulate debris tongue is a unique elongated landform among several lobate-shaped mass wasting units in the Eastern Hellas Planitia area. It is located in the southern Hellas Montes, north of the Reull Vallis at approximately 97.2°E and 39.0°S (figures 9.1 and 9.3). The area is generally characterized by an abundance of smoothly shaped remnant massifs and mounds that pierce through large lobate debris aprons consisting of complex assemblages of individual coalescing debris lobes. Such remnant massifs have been genetically related to the Hellas impact event and represent either crustal uplift or ejected material (e.g., *Greeley and Guest*, 1987; *Crown et al.*, 1992). The spatulate debris feature extends in NNW-SSE direction over a smoothly SSE-inclined surface pointing towards the Reull Vallis (dt in figure 9.3b).

Toward north of the debris tongue several conical-shaped remnant massifs (rm1-3 in figure 9.3b) are observed. Their bases are defined by several debris apron lobes emerging below these remnant massifs (al1-5 in figure 9.3b). The southern margins of a particular debris apron lobe (al3 in figure 9.3b) co-
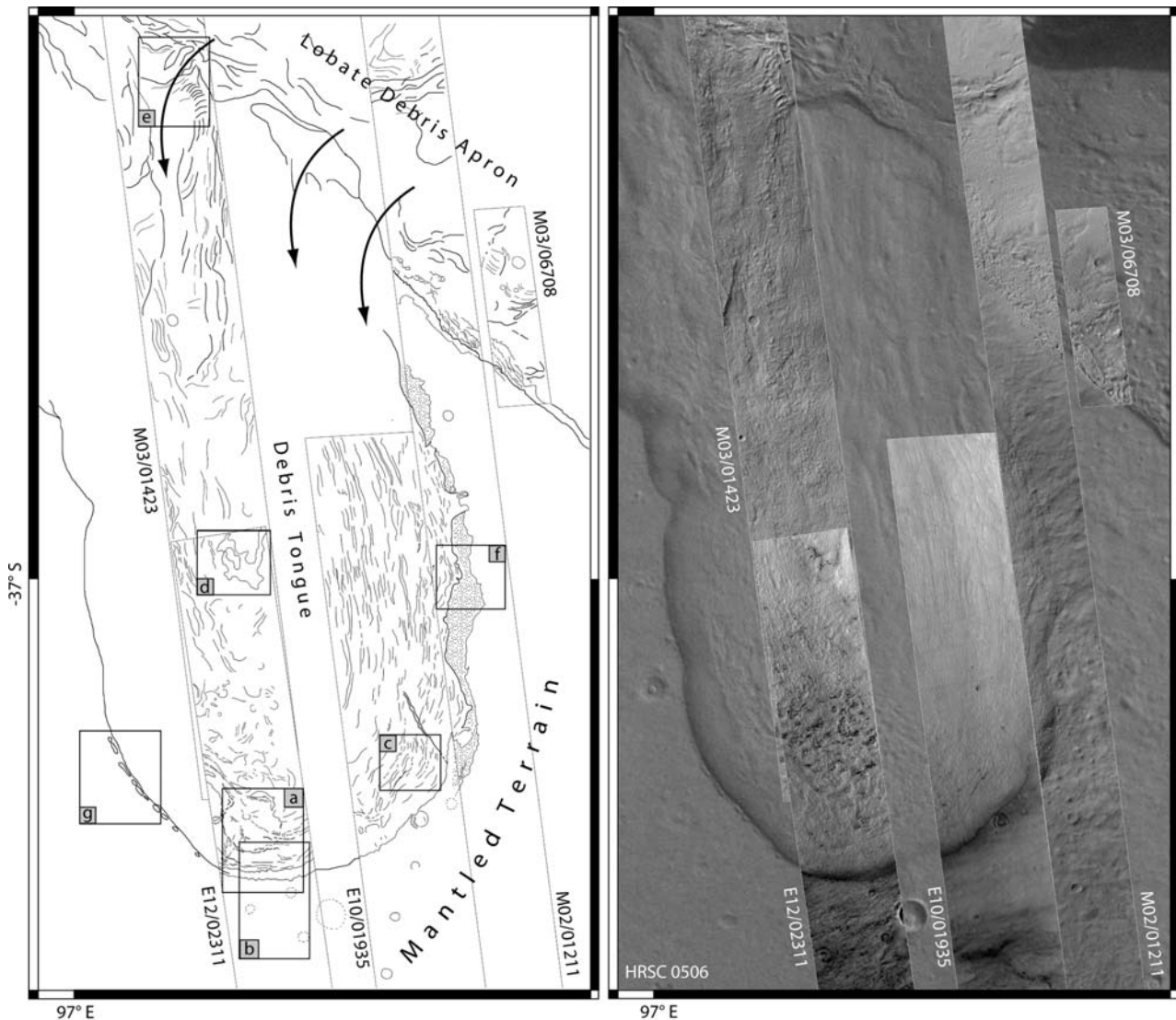
Figure 9.5.: Detailed ridge-and-furrow pattern and textural properties (left) as derived from MOC mosaic image data covering the spatulate debris tongue; MOC scenes superimposed on HRSC nadir scene of orbit 506 (right; Table 9.1). Mass transport indicated by arrows. Dotted area at eastern debris-tongue margin indicates smooth textured unit discussed in the text. Letter-labeled boxes refer to individual scenes in figure 9.6 and 9.7, for scale see figure 9.4, north is at top.

alesces with the northern parts of the debris tongue (dt). In conformal projection it becomes obvious that the eastern and western margins of the debris tongue slowly converge toward north and point to the inside of a large 32-km-diameter depression at 97°E, 37.5°S (figure 9.1).

Topographically, the debris tongue is only imprecisely represented by the gridded 128-pixel-per-degree MOLA-based MEGDR data available from the PDS Geoscience Node. Most precise individual mea-

surements have therefore been obtained using individual MOLA PEDR track data (see figure 9.4).

The top of the convex-shaped terminus of the debris tongue is situated on an elevation level of -2050 m whereas the top of the northern part of the tongue-shaped landform reaches an elevation of -2130 m providing a value for the total difference of relief of approximately 80 m in NS direction. Abutting marginal plains are on an elevation level of below -2200 m. The maximum debris-tongue thickness at the terminus is

Table 9.1: References to image data covering the Martian debris tongue.

Instrument	Image ID	Map Scale
MOC-NA	m02/01211	3.4 [m/px]
	m03/01423	5.1 [m/px]
	m03/06708	1.4 [m/px]
	e10/01935	3.5 [m/px]
	e12/02311	3.5 [m/px]
HRSC	0506/0000	25.0 [m/px]
	2510/0001	25.0 [m/px]
THEMIS	V16685001	17.0 [m/px]

approximately 150 m and less than 100 m at the northernmost location. The surface on which the debris tongue resides is slightly inclined to the SSE, therefore the thickness value at the terminus has to be considered as lower limit. The debris tongue itself has an asymmetric shape at its northern location with lower relief at the center and eastern margin (e.g., MOLA track ap13402 in figure 9.4). This asymmetry is also reflected by textural properties as expressed by several sets of elongated depressions on the surface of the debris tongue (figure 9.3a). Lateral and frontal margins are convexly shaped as indicated in all profiles that cross the debris apron (MOLA tracks ap11480, ap01578, ap12545, ap13402 in figure 9.4). In plan view, the western tongue margin is irregularly shaped and characterized by short outward-facing lateral lobes indicating a component of debris movement in western direction, i.e., perpendicular to the main transport direction (figure 9.3a).

At its broadest part, the debris tongue has a width of ≈ 16 km and a apparent length, i.e., the length between terminus and location of coalescence with the upper debris apron, of 26 km to 32 km. The effective length can not be determined visually due to obliteration caused by coalescence of debris apron and debris tongue. The area occupied by the observable part of the debris tongue is estimated to be ≈ 250 km² while earlier measurements say that "the area covered by the deposits is 325 km²" and a value of 170 km² for the "head of the debris flow" is provided (*Baratoux et al.*, 2002)).

Slight differences in relief between the western and eastern debris tongue are well reflected by the anaglyph view. Some of these topographic differences and undulations are also reflected by individual MOLA profiles (figure 9.4): The westernmost profiles (ap12545 and ap11480) are on slightly higher topographic level than the eastern profiles (ap12655 and ap13402) indicating either internal inhomogeneities of the debris or degradational modification after emplacement.
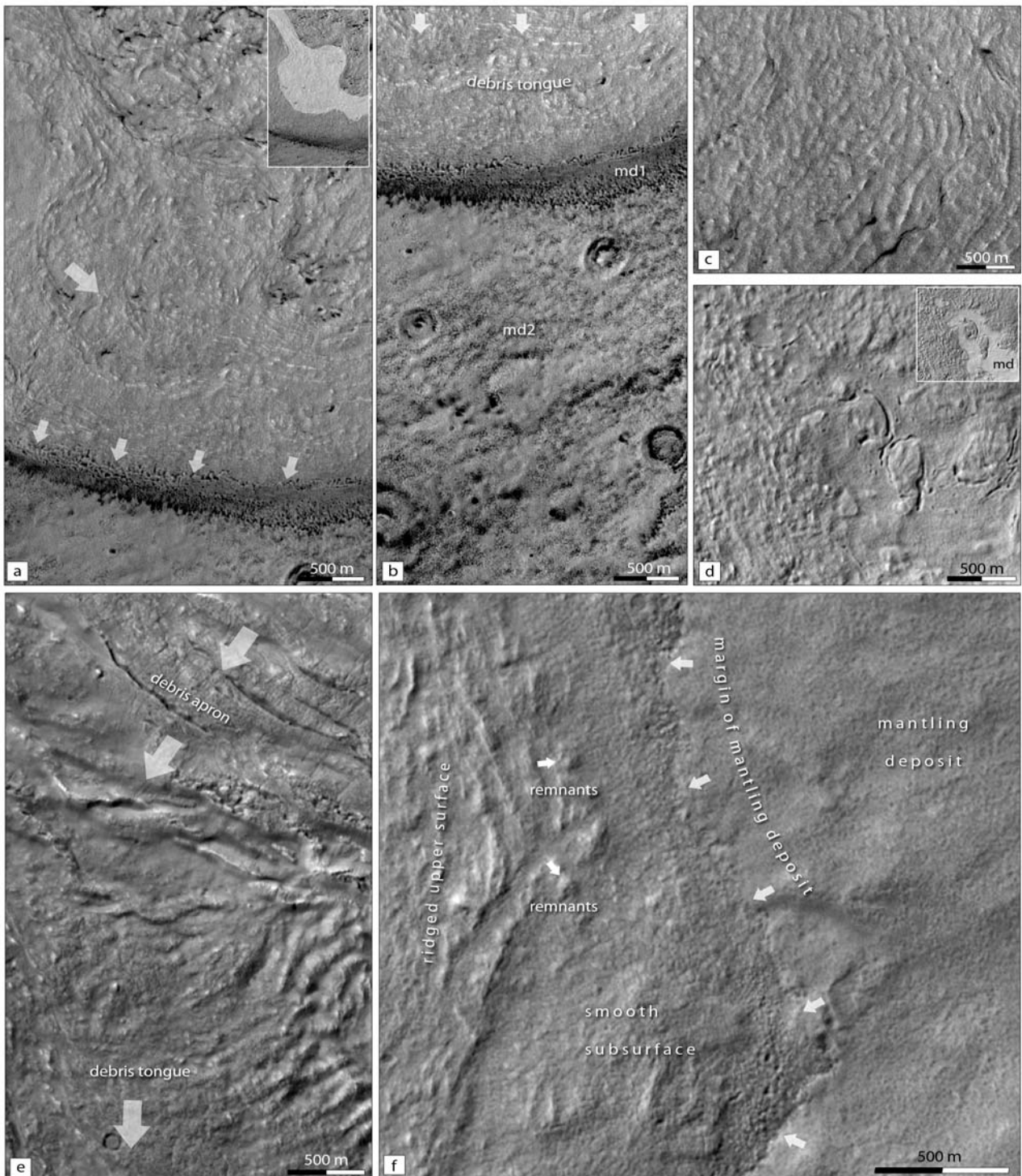
9.3.2. Textural Properties

The textural surface inventory and its zonal distribution among the debris tongue surface is roughly subdivided into a *pitted zone* and a *ridged zone* as stressed in the sketch maps (figures 9.3b and 9.5) and MOC image samples (figure 9.6). Although some of these textural properties can be diffusely observed at HRSC scale, only high-resolution MOC data provides full details and gives insights into fine-scaled surface characteristics.

Pitted zone: a pitted pattern is observed near the western snout of the debris tongue covering approximately 10% of the overall debris-tongue area. The pitted zone gradually vanishes in northern direction and merges with a linear ridge-and-valley pattern. This pitted surface type shows the most complex set of textural arrangements and features on the debris-tongue surface with chaotically arranged partly circular, elliptical or arcuate to sigmoidal shallow depressions. At MOC-NA resolution the observed patterns are formed by numerous overlapping and coalescing surface flows which cause an undulating topography through complex arrangements of compressional ridges and arcuate furrows (figures 9.5 and 9.6a). The

least degraded flow unit (brightened area in inset in figure 9.6a) forms two arcuate 400 m wide bands parallel to the main debris tongue margins which meet in a circular-shaped catchment area forming a chaotic assembly of ridges and furrows. The two coalescing bands show flow-parallel ridge-and-furrow patterns. *Ridged zone:* in upstream direction towards north, pits and hollows vanish gradually or become elon-

gated producing a lineated ridge-and-valley texture which is oriented parallel to the debris-tongue margins (figure 9.5). This texture pattern continues towards the northernmost zone where it gradually rearranges with a ridge-and-valley texture that is perpendicular to the debris tongue margins and which is obviously generated by the coalescence of lobate debris apron and debris tongue (figure 9.6e). A characteristic degradational feature of the ridged zone can be observed at the eastern tongue margin (dotted fill pattern in figure 9.5). A narrow band with a smooth texture extends from north to south and connects the ridged surface of the debris tongue with a mantling unit on abutting units. This smooth zone covers approximately 5% of the debris tongue (figure 9.6f).

9.3.3. Margins and Frontal Terminus

The frontal part of the debris tongue has a generally symmetrical shape and is sharply delineated by an arcuate terminus which separates the debris-tongue unit clearly from the surrounding plains (figure 9.3). Topographic profiles crossing the debris tongue's terminus are highly convex upward and similar to those profiles observed at margins of lobate debris aprons (e.g., *Squyres*, 1978; *Squyres and Carr*, 1986; *Mangold et al.*, 2002). Terminal ridges and furrows are densely spaced and are oriented parallel to the main debris tongue margins. At closer inspection, a terminal ve-

neer becomes visible that is partly draped over the frontal steep margin of the debris tongue (figure 9.6b and arrows in figure 9.6a). This veneer has a degraded fretted appearance and is superimposed on the main debris tongue material (md1 in figure 9.6b). At the lower kink, the thin veneer is overlain by a brighter deposit which is less dissected (md2 in figure 9.6b). This observation is not caused by illumination conditions as confirmed farther towards south where a mantling deposit md2 (figure 9.6b) is partly dissected and reveals lower strata md1. We can observe such a layer at the terminal plains and also in the interiors of impact craters.

A third observation covers the western terminal margin (figure 9.7), where THEMIS as well as HRSC image data show well pronounced and aligned elongated knob-like features at a size of a few tens of meters and up to one hundred meters. These knob-like features do only occur at the western margins and have no counterparts at any other location of the debris tongue.

The western margin of the debris tongue is not covered by any high-resolution MGS-MOC image data so that we have to concentrate on the eastern margin which is also closer to the terminal parts of the northern debris apron lobes (figures 9.1-9.3). Details of that margin are displayed in figures 9.5 and 9.6f.

Here, at least three units can be distinguished. First,

Figure 9.6.: (opposite page) high resolution MOC scenes (a-f) of characteristic surface textures of the debris tongue. Labeled boxes refer to location marked in figure 9.5. [a] Turbulent and laminar flow pattern on the surface of the debris tongue indicating post emplacement modification by surface flow similar to terrestrial supraglacial rivers. Area of surface flow is brightened in the inset view at top right. [b] Southern debris-tongue margin showing fretted mantling-deposit blanket at snout. Different mantling deposit units are indicated by changes in relative albedo (md1 and md2). [c] Ridge pattern parallel to debris tongue margin indicating shear strength and deformation similar to (rock) glaciers. [d] Smooth surface unit eroded into the debris-tongue surface indicating degradation. Inset shows area brightened to aid visibility. [e] Northern coalescence zone between lobate debris apron and spatulate debris tongue. Note, changing orientation of compressional ridges indicating contemporary deformation of both units. Arrows indicate main mass transport direction. [f] Eastern debris-tongue margin. Degradation of the upper debris-tongue layer (arrows pointing left) caused exhumation of a smooth underlaying deposit. Several remnant blocks (arrows pointing right) of the ridged surface are disconnected from the upper layer and tilted. The eastern margin of the smooth deposit is overlain by thick mantling deposit with eroded and fretted margins. North is always up, illumination is from top left
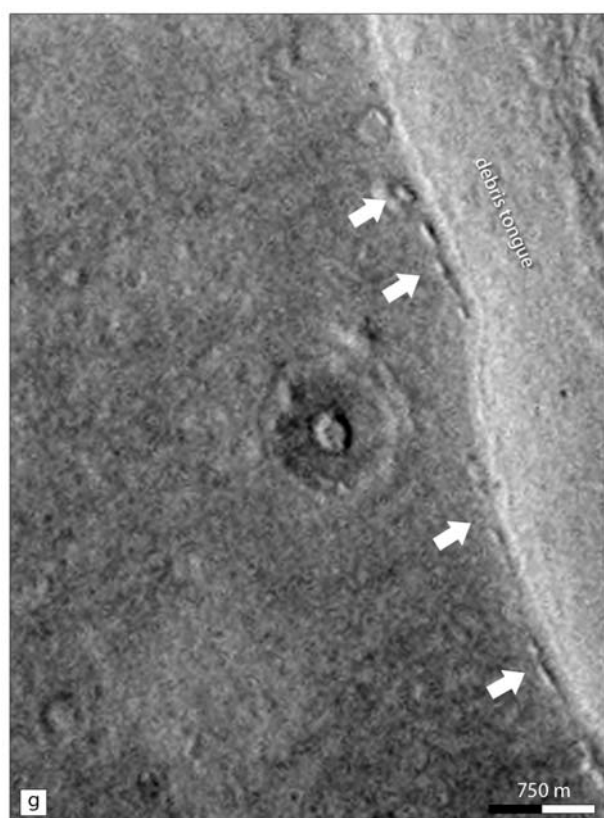
Figure 9.7: Eroded elongated knobs (arrows) parallel to the western debris-tongue margin indicating either relics of former uplift of plains material during advance of debris tongue similar to glaciotectonic processes or remnant material that fell down the debris tongue comparable to glacial drop moraines. THEMIS scene V16685001, for location see figure 9.5, north is at top, illumination from the bottom left.

a unit on top of the debris tongue that is characterized by elongated ridges and furrows parallel to the direction of tongue movement (ridged upper surface in figure 9.6f).

Secondly, there is a smooth textured unit at the eastern margin of the debris tongue (smooth subsurface in figure 9.6f). Several apparently rotated remnant blocks showing characteristics of the upper unit are located inside this smooth unit.

Thirdly, a smooth and slightly undulating surface texture covers the smooth subsurface unit from the east. The border of that unit is fretted and dissected (arrows in figure 9.6f). The extent of the intermediate eastern unit is mapped on MGS-MOC data and displayed in figure 9.5.

The alleged debris tongue's root zone as defined by the southern boundary of the lobate debris apron al3 and the northern part of the debris tongue (dt in figure 9.3b) shows some unusual pattern and changes in main direction of ridges. The transition of debris apron and debris tongue itself is morphologically

characterized by a change of the ridge pattern, i.e., a transverse ridge-and-furrow pattern on the lobate debris apron and a ridge-and-furrow pattern parallel to the elongation of the debris tongue (figure 9.6e). This zone is relatively diffuse as the narrow spacing of ridges and furrows produces a complex overlapping pattern between apron lobe (al3) and debris tongue (dt) where individual structural units cannot be unambiguously attributed to either the debris tongue or debris apron.

As reflected in topographic data (figures 9.3, 9.4a), the debris apron lobe (al3) is at least partly superimposed on the debris tongue (dt). Image data suggest that debris-apron material has been pushed partly onto the debris tongue forming new sets of compressional ridges.

This observation is stressed in a sketch characterizing transverse depressions (filled areas in figure 9.3). The characteristic sub-parallel pattern of transverse depressions becomes more dense toward the contact of both, debris apron unit and debris tongue.
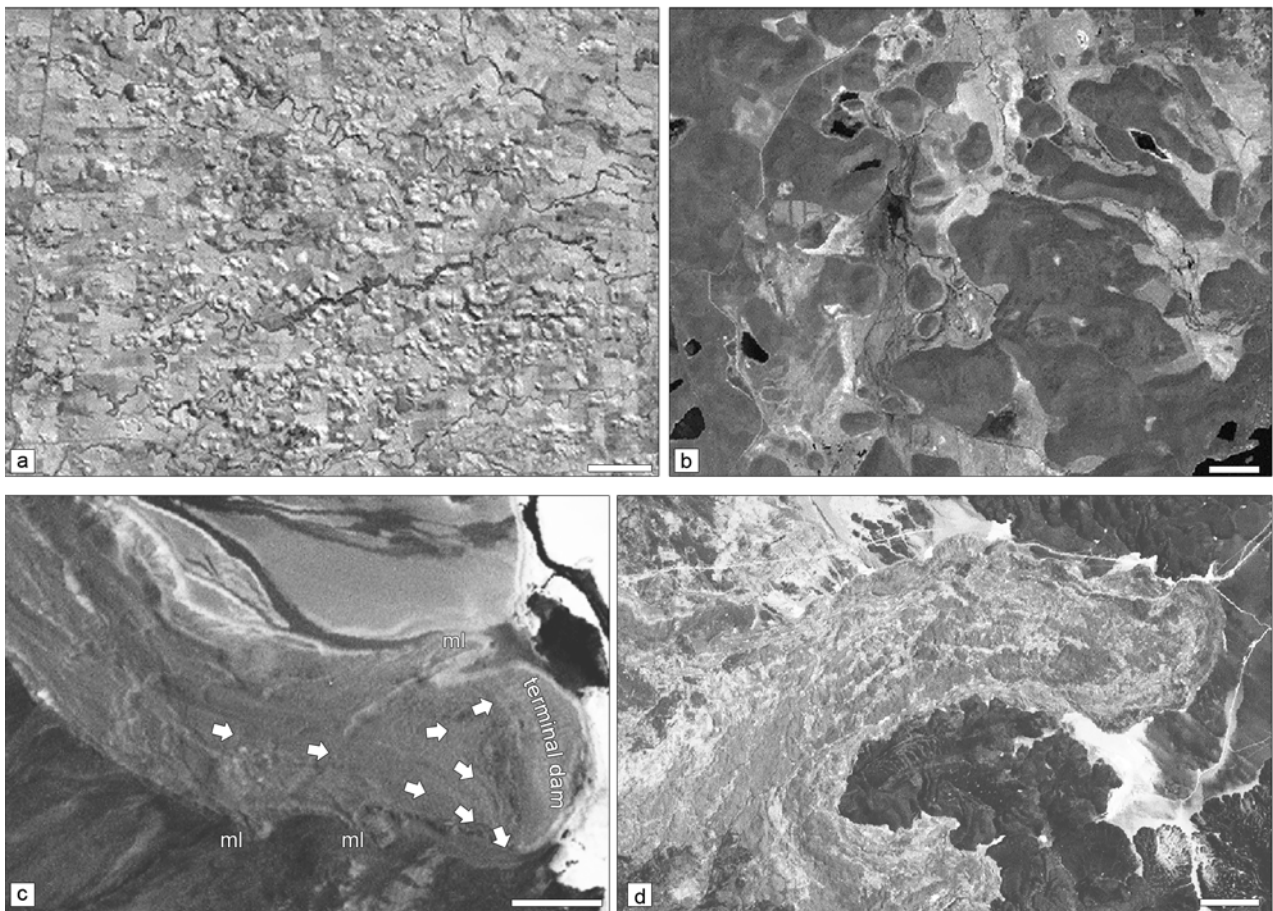
Figure 9.8.: Examples of terrestrial volcanically derived debris avalanches. [a] Hummocks derived from wave propagation of debris during debris-avalanche emplacement, western Mt. Taranaki, North Island, New Zealand, 173°53'E 39°17'S, ETM+ p073r087. [b] Large wave-propagation hummocks, pleistocene debris avalanche caused by volcanic sector collapse, Mt. Shasta, northern California, 122°26'W 41°33'N, ETM+ p045r031. [c] Debris avalanche with marginal lobes (ml), terminal dam and diverging lines of debris transport at dam (arrows), eastern Llullaillaco, Argentina, 68°20'W 24°50'S, ETM+ p233r077. [d] Secondary Socompa debris avalanche showing irregluar shape with marginal lobes, broad terminus and chaotically aligned surface features, Chile, 68°17'W 24°06'S, ETM+ p233r077. North is always up. Scale bar is 1000 m.

9.4. Interpretation

9.4.1. Style of Emplacement and Microrelief

The complex coalescence pattern at the contact of the debris apron and the northern part of the debris tongue are problematic to interpret as ridges and furrows can not be unambiguously attributed to either landforms. The change of direction of ridges and furrows strongly suggest ongoing creep processes at a time when both units have already been emplaced, consequently, units are superimposed onto each other. This view is also supported as ridges and furrows are spaced more densely towards the contact of both units indicating compression or even overthrusting of debris material that has been pushed from the debris apron onto and into the spatulate landform. These complex forms of ridges and furrows are characteristic of terrestrial rock glaciers and have been extensively studied in the past (e.g., *Wahrhaftig and Cox*, 1959; *Barsch*, 1996; *Kääb and Weber*, 2004).

The smooth texture observed in the two bands of the intermediate part of the debris tongue (figure

Figure 9.9: Remnant knobs as possible source for debris tongue as proposed by *Baratoux et al.* (2002). Arrows indicate direction of mass transport through several valleys. Smooth shape and small incisions indicate slow processes. No traces can be observed that suggest catastrophic collapse or other mechanisms that would allow formation of the large debris tongue (dt), for location see figure 9.3. HRSC scene from orbit 2510, north is up, illumination is from top right.

9.6a) suggest laminar flow conditions while the central catchment area is characterized by patterns indicative of turbulent flow. Such patterns can often be observed on debris-covered glaciers (or other debris transport systems) which can be resurfaced by supraglacial drainage (e.g., *Benn and Evans*, 2003, p. 237ff) or debris reworking and englacial rivers (e.g., *Menzies*, 2002, p. 159). The presence and alignments of relatively well preserved ridges and furrows indicate at least a considerable shear strength inside the debris tongue which disqualify Newtonian flow conditions. Alignments of ridges and furrows are in principle parallel, i.e., longitudinal, to the debris-tongue margins. The parallel alignment of ridges and furrows and compressional features at the terminus indicate slow rock glacier-like deformation conditions that affected the complete debris body. Primary debris-tongue advance probably occurred during a single short - or perhaps longterm - event rather than by gradual advance of individual debris-lobe units with phases of stagnation. Besides the homogeneous overall appearance and the continuous ridge pattern this observation is additionally confirmed by the fact that overlapping individual debris lobes that are characteristic of terrestrial systems could not be identified (e.g., *Wahrhaftig and Cox*, 1959; *Haeberli*, 1985; *Vitek and Giardino*, 1987; *Barsch*, 1988, 1996).

The frontal terminus of the debris tongue as well as the eastern and western margins show several characteristics indicating a complex emplacement, deformational and erosional history. The symmetric plan-shape implies flow or creep of a medium with considerable yield strength and a significant internal cohesion which did not allow formation of marginal lobes of significant size. The highly convex-upward terminus compares closely to margins of lobate debris aprons (e.g., *Squyres*, 1978; *Squyres and Carr*, 1986; *Mangold et al.*, 2002) and therefore indicates a similar style of emplacement (figure 9.4). The overall concave shape is often observed at terrestrial degraded and fossil rock glaciers and does not necessarily allow to draw conclusions on the rheology (e.g., *Ikeda and Matsuoka*, 2002; *Berthling et al.*, 1998). However, it is indicated by this profile that the landform is currently not active and might be even fossil. Most of the narrow flow-parallel ridge patterns are dissected (figures 9.6b-c, 9.6e-f) suggesting post-emplacement degradation. Filled quasi-circular depressions on the surface of the debris tongue that can be observed farther to the north (figure 9.6d) indicate loss of volume in the subsurface and/or subsequent subsidence of the upper surface, i.e., thermokarstic processes.

It appears that the thickness of the debris tongue reaches its maximum at the terminus which has been

explained by *Baratoux et al.* (2002) through formation of a terminal dam often observed at terrestrial avalanches (e.g., *Iverson et al.*, 1997; *Iverson*, 1997). A terminal thickening can generally be explained by high energetic masses that have been mobilized and accumulated as larger blocks at the fronts. Later propagation waves of debris then accumulate at the dam and aid increasing its size (e.g., *Iverson*, 1997). Natural obstacles at the flow terminus are another possibility for dam formation. When a dam forms, flow lines diverge in front of the dam as subsequent debris waves flow around the obstacle. Such a dam can not be observed at the Martian feature as the thickness of the debris tongue increases gradually from the apparent source to the terminus. The compressional pattern that can be traced throughout the debris body is coherently parallel to the margins. An additional observation that speaks against a terminal dam is that no large boulders or blocks which might form the terminal dam are observed, in contrast, the overall surface is generally quite homogeneous throughout the main debris body. Indications for wave propagation topography such as a hummocky surface with chaotically to sub-parallel aligned hills and ridges is also not observed (figure 9.8a-b) although these features are relatively common for debris avalanches observed on the Earth (*Brantley and Glicken*, 1986; *Crandell*, 1989; *Glicken*, 1996; *Christiansen*, 1982; *Crandell et al.*, 1983, 1984).

The peculiar alignment of knobs at the western debris tongue margin might also indicate degradational processes although the coarser image resolution when compared to MOC scenes does not allow us to provide more than speculations on their origin. The alignment might indicate an upturning of strata at the terminus of the debris tongue that took place during advance of the debris tongue. Plains material has been compressed and was partly pushed against and draped over the snout of the debris tongue similar to glaciotectonic processes (e.g., *Menzies*, 2002; *Benn and Evans*, 2003). This explanation requires observations of compressional patterns all around the terminus which we cannot confirm. Alternatively, disintegrated surface material might have fallen from the de-

bris tongue during its advance. This process is comparable to formation of terrestrial glacial drop moraines where during glacial retreat or advance incorporated debris falls from the glacier and delineates a zone of glacier presence. This ridge of eroded surface material now disintegrates and leaves behind remnant relics at locations protected from constant sunlight. The fact that they only exist in a shadow zone at the southwestern margin of the debris tongue supports this theory and indicate volatiles or ice might be involved. Although more convincing than the first alternative, formation of such large coherent piles of material by accumulation of degraded mantling material remains questionable. A definitive answer might only be found through higher-resolution data.

The insights we obtain through the differently textured layers in the eastern part of the debris tongue (figure 9.6f) suggest a layered composition of the debris tongue and provides evidence for the degradation of the landform. When interpreting the three different units consisting of the topmost ridged layer, the intermediate smooth layer and the mantling in the East it becomes obvious that this smooth intermediate unit is most probable a degradational remnant unit that became visible when the upper surface was subject to disintegration and degradation. At the relatively steeper margins the upper ridged surface material was mobilized by gravitational block gliding and rotation. Apparently, most of the disintegrated material is reworked into unconsolidated debris which is collected at the footslope as indicated by the slightly rougher surface texture. Degradation of a surficial layer is also suggested for the veneer that is draped over the terminal debris tongue (figure 9.6a-b). Its fretted appearance clearly indicate disintegration of thin layer that has once may have covered larger areas of the terminus.

9.4.2. Source Area and Origin

In order to understand the true nature of the tongue-shaped landform discussed herein it is inevitable to identify its source area and mechanisms that have led to its formation. What we can observe thus far is that
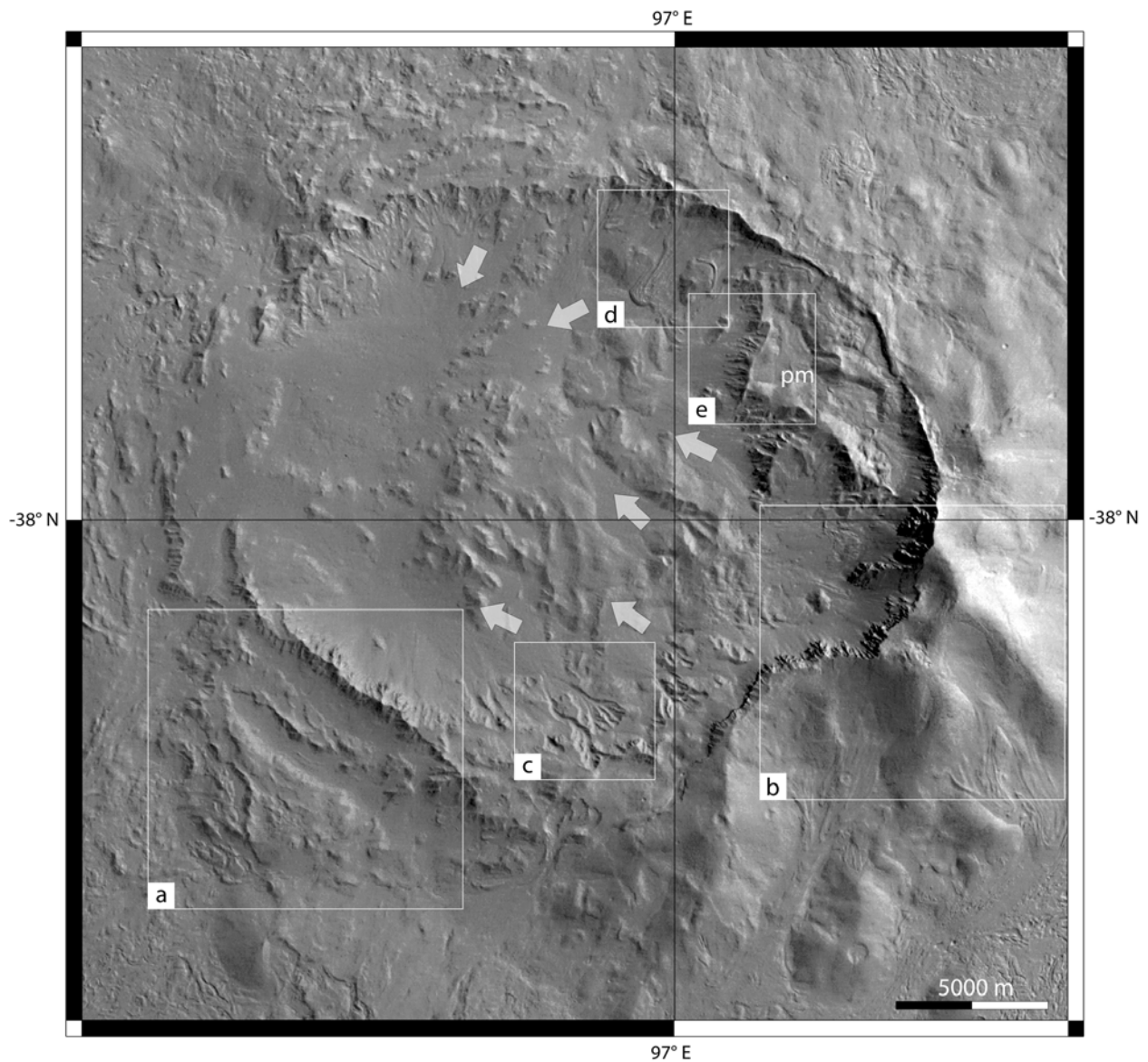
Figure 9.10.: Putative degraded caldera in eastern Hellas Planitia and source of various landslide units in the west and south. Arrows indicate directions of mass transport, promontory (pm) in the northeast is considered to be a remnant of the former interior floor. Labeled boxes refer to scenes in figure 9.10. HRSC scene of orbit 2510.

the debris tongue is covered by younger or contemporary units which have contributed to (a) deformation and (b) obscuring of the original scenery. It is suggested that the remnant massifs which have been proposed earlier as possible origin by *Baratoux et al.* (2002) are not likely to have contributed significantly to debris-tongue formation for two reasons:

One explanation has been given by the authors themselves as the sizes of the remnant massifs are simply to small. If the debris tongue is considered to have formed during a single event, it could have been formed only if the remnant massifs that have been proposed as source have collapsed instantaneously.

The smooth shape which is visible today would have been formed during later erosional activity. This scenario is unlikely as we cannot observe traces for sudden remnant collapse and material supply of the size of the debris tongue. The possibility of long-lasting

rock-fall activity as discussed in literature and considered for debris apron formation is excluded from further discussions on possible formation mechanism as the landform's shape shows no indications for long-lasting supply and steady advance. The proposed two remnant knobs are more likely degradational relics derived from an isolated remnant knob similar to adjacent features. It was shaped by marginal as well as surficial debris flows and similar mass-wasting processes. Flow and sediment transport or even rock fall have cut a radial network of intramountainous valleys into the remnant's surface. This configuration is the result of a long-lasting process and it is obvious from observations of image data that these processes contributed to formation of the large debris apron. However, a direct link between these processes and debris-tongue formation is missing as the heavy erosion of the remnant knob is not reflected in the current much less degraded appearance of the debris tongue although both landforms were exposed to erosional processes for the same time. If debris apron and debris tongue are considered to be roughly of the same age and the remnant massif has contributed to the formation of the debris apron by the processes now seen, it remains unexplainable when the large-scale collapse of the remnant massif should have taken place.

Secondly, geometrically the alleged remnant knobs are not located in the projected main direction of the tongue-shaped unit but are offset toward the east. These settings can be roughly estimated by extrapolating two lines delineating the debris tongue in the direction of the source area. Theses lines converge toward north but do not meet with the remnant knobs, instead they cut near the center of a large 32 km diameter depression (figures 9.1, 9.9 and 9.10). A similar method has been described by *Francis and Oppenheimer* (2004, p. 302f) for estimating the area of a tongue-shaped debris avalanche. The proposed debris avalanche that has formed by collapse of the proposed remnant knobs must have changed its path directly near the source area which is considered to be unlikely if we assume a high-energy/high-velocity and sudden mass transport characteristic of

avalanches. Even if a slow emplacement style was considered there are no indications that the topography of the subsurface has forced the debris tongue to remain in a confined bed. Based on these observations we conclude that the possible root zone of debris tongue material is located within or near the large depression in the north that has been mapped as an impact-crater structure in earlier work (e.g., *Greeley and Guest*, 1987; *Crown et al.*, 1992). There are, however, several observations that cast doubts on the nature of this depression; these are discussed hereafter in more detail.

Near-to bowl-shaped depressions with elevated rims, a central peak-like mound and a roughly circular shape (figures 9.10-9.11) are generally primary indicators for identifying an impact crater structure. The depression proposed as source area for the debris tongue shows several indications that suggest a volcanic rather than an impact origin:

Rim appearance: The appearance of the depression rims (figure 9.10) varies in shape and preservation. In the east and north rims have a pristine and sharply defined appearance whereas the southern and western rims are highly degraded or show traces of stair-stepped wall-rock failure and collapse (figure 9.10, 9.11a). Even more confusing is the fact that although parts of the rims look relatively undegraded, the alleged impact crater itself is rather old as it shows substantial traces of degradation at its interior and surrounding terrain. From the state of preservation at the interior one would expect smoothly shaped and eroded rims in the north and west. This setting is unusual for impact-crater structures but is usually observed at locations, where sudden wall-rock failures, e.g., caused by headward erosion and over-steepening, occur. Such large-scale failures are usually attributed to processes triggered by intense weathering or endogenic forces. Although rim collapse of impact craters do not occur frequently as the impact event forms stabilized wall rock through the excavation process, less pronounced features can be observed at very few places on Mars. The eastern rim is sharply defined towards the interior and smoothly shaped and less pronounced towards the exterior (fig-
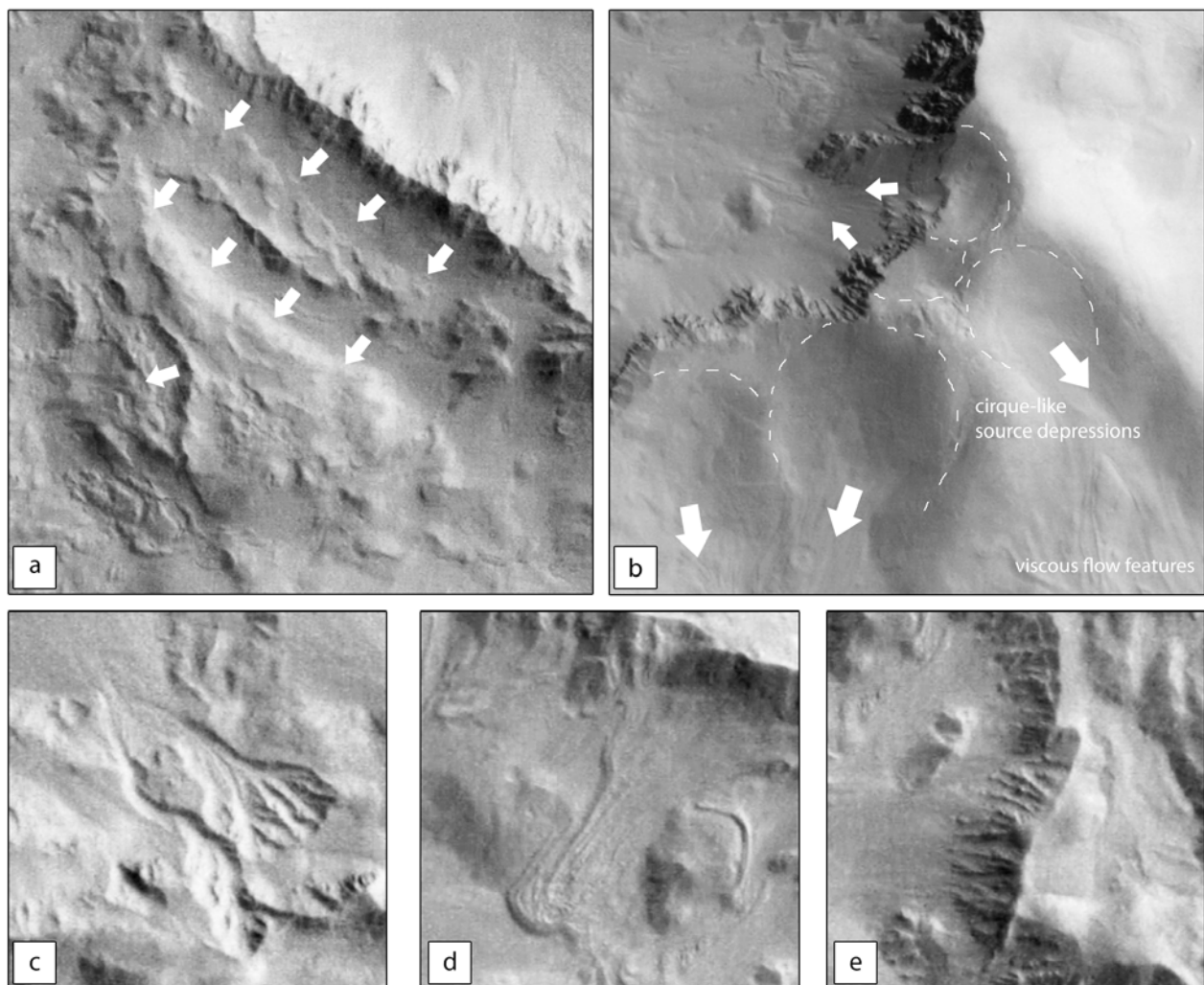
Figure 9.11.: HRSC scenes from putative volcanic construct. Labels refer to locations in figure 9.10. [a] stair-stepped rim indicative of wall-rock failure, scene width is 10.5 km; [b] eastern rim of the caldera-like depression. Rims oriented towards the interior are sharply delineated, outer rims are smoothly shaped. Rims are characterized by cirque-like depressions that form the source of viscous flow features, scene width is 10 km; [c] Gullied slide flows on the interior depression floor are situated on different elevation levels. Several alluvial fans are incised by younger slide flows, scene width is 4.7 km; [d] Viscous flow features at the northern depression rim, scene width is 4.4 km; [e] Rims of the remnant promontory at the northeastern depression wall, scene width is 4.1 km. North is at top in all scenes, sun illumination is from top right.

ure 9.10). The outer rim is dissected by cirque-like features that are source of elongated surficial flow units such as viscous-flow features as well as broad debris lobes (figure 9.10, 9.11b, 9.11d). An impact-event that excavates such a depression would have covered much of the exterior topography with ejected material and would not have cut a clear and sharply defined scarp into pre-existing wall-rock. What has been interpreted as impact-crater rim might also be a former remnant massif that has formed during the Hellas impact event (*Greeley and Guest*, 1987).

Interior promontory: An unusual spur-like promontory resides at the inside of the northeastern rim of the depression (pm in figure 9.10 and 9.11e). Unusual about this setting is that an impact event normally excavates material but does not leave behind remnants where the excavation occurs. However, post-impact degradation and subsequent failure such as
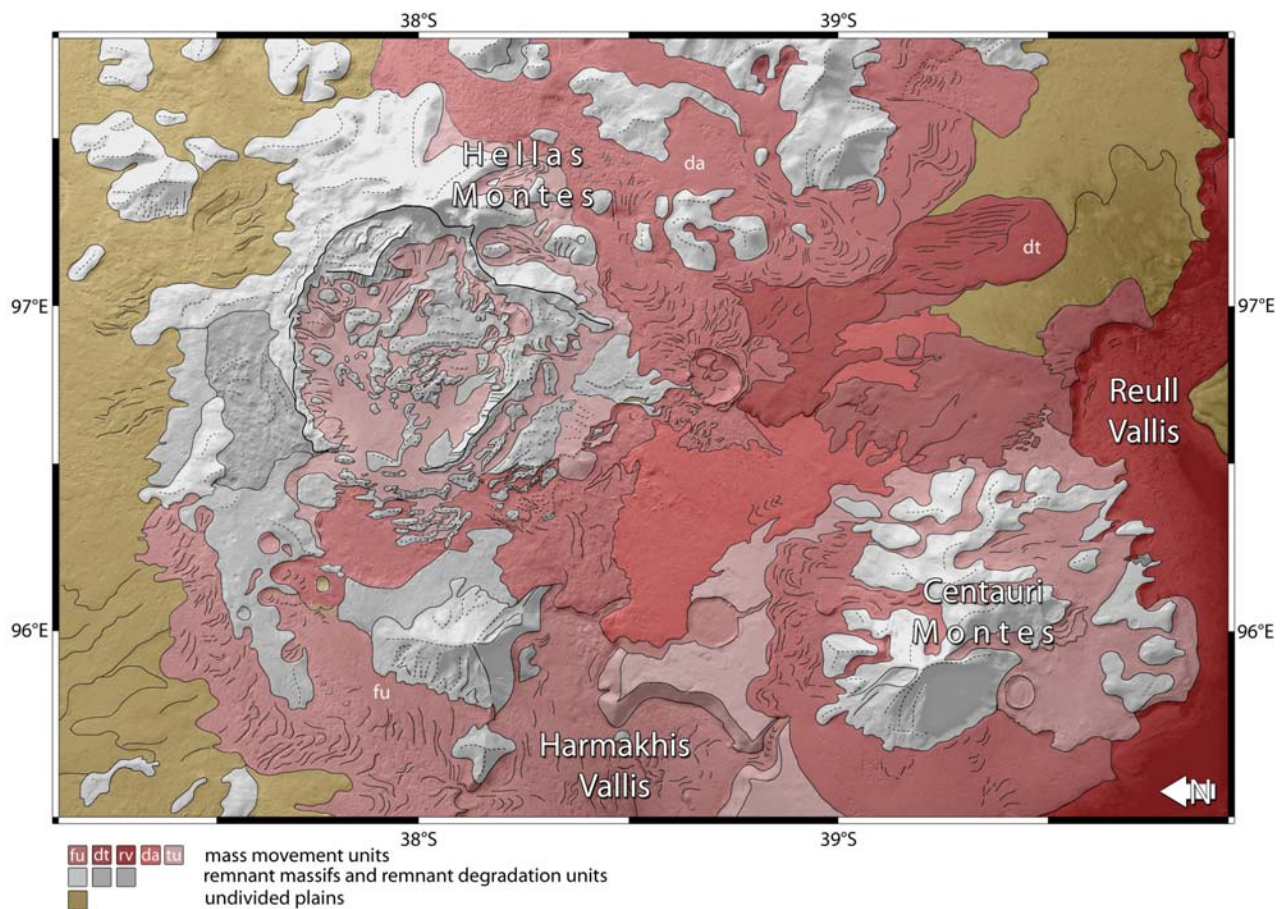
Figure 9.12.: Geomorphic map of the study area. Landslide units are colored in red tones: Harmakhis (Centauri/Hellas Montes) flow units (fu), debris tongue (dt), Reull Vallis unit (rv), Hellas Montes debris apron (da), other flow units (tu). Remannt massifs (bright) and degraded remnant massifs (dark) are in gray colors. Undivided plains have brown colors. Solid lines indicate vorders and flow patterns, dashed lines refer to hill crest lines. North is to the left. Mapping has been performed on stereo data derived from the nadir and stereo-1 channels of HRSC orbit 2510. For comparison reasons left is towards the left as in figure 9.1.

block-slidings could be one explanation although the lack of evidence at other locations within the depression make this explanation more unlikely. The eastern crater wall looks intact however and there is no indication of block movement which could explain this promontory. Moreover, the block margins pointing inside have a peculiar arcuate shape which could indicate margins of former elliptical to circular features such as former caldera-wall rims.

Mass wasting: The chaotic assembly of material on the interior floor of the depression is unusual when compared to other impact-crater structures common on Mars. Although impact-crater floors often show remarkable traces of their depositional post-impact history which might consist of deltaic or alluvial fan deposits, dune fields, lava flooding or surficial mass wasting processes, the interior of this very depression clearly indicates directional mass transport from the eastern rim towards the west.

Landforms indicative of intense mass wasting at this location consist of numerous occurrences of sub-parallel gullied-slide flows and terminal depositional fans that reach from higher elevated levels of the depression in the east to the more obliterated western rim (figure 9.11c). Additionally, several landslides and viscous flow features originate at the in-

terior rims and contribute to significant mass transport downslope toward the interior of the depression. They accumulate near the center of the depression forming a chaotic mound-like feature that roughly resembles a central peak. Flow and creep features are also observed at the eastern outer rims (figures 9.11b, 9.11d). There are traces that most of the interior mass-wasting material has been removed from the center and the western rim toward a southern direction during multiple events. Material from the interior and the former western rim accumulated south of the depression. Here, mass-wasting material coalesces with wall-rock material derived from the Centauri Montes remnant massifs in the south (figure 9.12). These deposits have been mapped out on the basis of textural properties and on the basis of stereo data that clearly showed different levels of superpositions. However, the assemblage of various landslide units is rather complicated and chaotic at several places which makes a clear separation of geomorphologic units awkward (figure 9.12).

Morphometry: Based on comparisons with morphometric data derived by *Garvin and Frawley* (1998); *Garvin et al.* (1999, 2000a,b) on the basis of MOLA topographic data for a global set of impact-crater structures on Mars it seems significant that most of the morphometric values obtained for this depression are significantly out of range (figures 9.13-9.14). Two representative MOLA profiles have been selected which cross the central peak and outer rims. Mean rim heights for Martian impact craters of comparable size, i.e., approximately 30 km - 35 km, as provided by *Garvin et al.* (2003) are in the range of 150 m to over 400 m. Heights of rims of the discussed depression are over 1000 m indicating that we are not observing a common rim feature but the former relief of the surrounding remnant topography in which the depression is incised. A central peak in an impact crater structure has a mean height of approximately 200 m. The observed central mound at the Hellas Montes depression has a height of about 800 m indicating a different origin. Moreover, both, rim height and central peak heights are far more larger than predicted even for the largest impact crater structures on

Mars (figures 9.14). Such large values are contradictory to what would be expected for a highly degraded impact crater structure which was filled by erosional debris. The depth of the depression is approximately 650 m and is one third lower than predicted for Martian impact-crater structures which gives an additional clue that the nature of the depression is different from an impact origin. It is obvious that erosional processes filled the interior of that depression which could explain lower depth values if an impact origin is considered. It would remains unclear why the height of the central mound should then be much larger than suggested by mean values of martian impact structures. Except for the central peak diameter of approximately 1000 m, all values are out of range and indicate another origin for the depression.

Geomorphologic context: An argument which is not based on direct observations but rather an argument based on the geomorphologic context is that the head region of the Harmakhis Vallis outflow channel is situated directly at the former western depression rim (figures 9.1 and 9.12). If the idea of outflow-channel formation through possible volcanic activity and melting of ground ice is considered to be true, the depression feature discussed herein could be interpreted as volcanic construct that has led to the formation of Harmakhis Vallis early in Martian history. It can be observed that large amounts of debris from areas adjacent to the depression flowed into the Harmakhis Vallis and it remains to be discussed in future work (a) in which way any volcanic activity at the discussed depression caused outflow channel formation, and (b) in which way outflow channel formation caused collapse of a volcanic construct which led to subsequent infill of Harmakhis Vallis.

We consider the given arguments as strong indicators for a volcanic origin rather than an crater-impact origin for the 32-km depression but still we can not completely rule out that intense mass-wasting processes caused modification of an old impact crater structure. Nevertheless, rim collapse is the major process which produced significant amounts of debris in surrounding areas which contributed to formation of the tongue-shaped features as well as a variety of
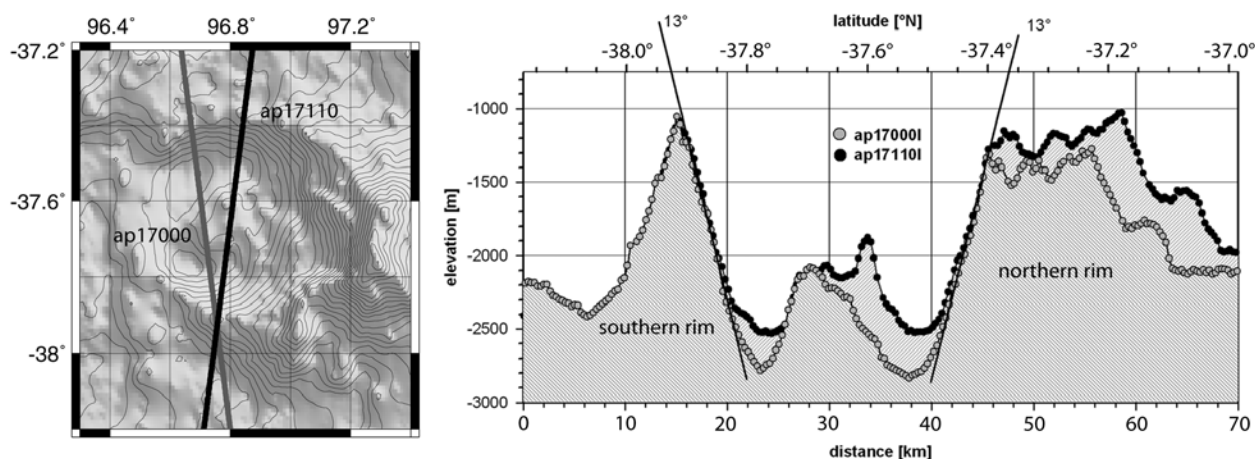
Figure 9.13.: Profiles as obtained by individual MOLA tracks. Shaded relief map on left shows location of MOLA tracks and terrain model representation by interpolating available MOLA tracks. Right figure shows cross profiles over the depression and the central-peak unit. Slope angles are approximately 13 degrees and are slightly lower than those of Martian impact craters as provided by e.g., *Garvin et al.* (2003).

other mass-wasting and creep-related landforms in the vicinity. The complex assemblage of various geomorphologic units makes any assumptions on the time of formation and interdependences of processes problematic, several constraints however allow us to give a rough outline of the sequence of events.

9.4.3. Sequence of Events

The transitional coalescence of compressional patterns and mixture of debris material between both creep units, lobate debris apron al3 and spatulate debris tongue dt, make various scenarios for the time of debris-tongue formation and conceivable. Apparent slightly different rheologies of both mass-wasting units are considered to be an important constraint when discussing the development of the debris tongue. These differences are not only reflected by the general shapes of debris aprons and debris tongue but also by the alignment of ridges and furrows. While on debris aprons transverse ridges are prevailing, ridges on the debris tongue are longitudinal. Both characteristics, shape and alignment of ridges, suggest significant differences in volatile content and allow some discussions on different scenarios:

[1] The debris tongue was emplaced before considerable masses of debris apron material moved south-ward and were pushed against and onto the debris tongue. In this case, the pattern of coalescing debris could have been formed only if the debris tongue contained enough volatiles to be deformed in a viscous manner (figures 9.3 and 9.6e). Debris apron material as well as debris material of the tongue-shaped landform were subject to creep deformation concurrently. This scenario does not suggest identical rheologies of both units but it allows mixture of different units at the zone of coalescence which implies compositional properties which are comparable to a certain degree. This scenario is not unlikely although we would expect a prominent topographic signature caused by the debris tongue underneath apron lobe al3 which could still be traced nowadays. On the other hand it can be easily imagined that ongoing deformation and advance wiped out any topographic signatures.

[2] If the debris tongue formed concurrently or shortly after emplacement of apron lobe al3, there is no other explanation than that the debris tongue originates directly from the main debris apron lobe al3 itself. This scenario implies that there must have been a significant release of volatiles and debris from the apron which aided debris tongue formation. Moreover, the different expressions of shapes imply that the debris tongue must have received considerable
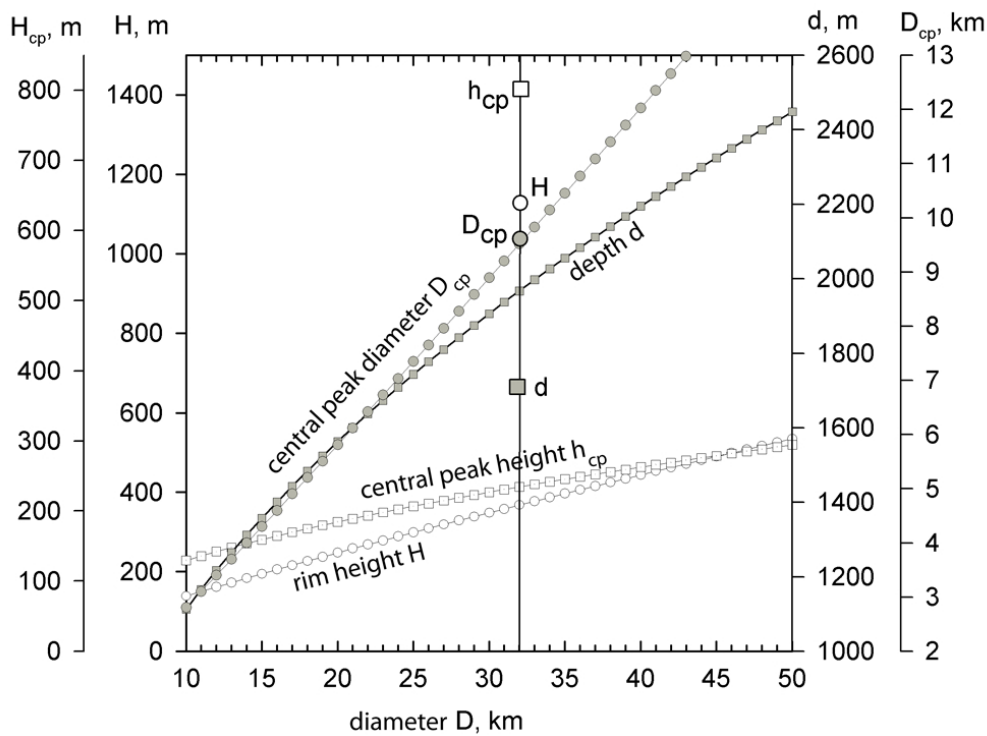
Figure 9.14.: Morphometric values derived by *Garvin et al.* (2003) for impact craters on Mars shown as curves. Discrete measurements of the Hellas Montes caldera are obtained through individual MOLA profiles. Parameters discussed are diameter (D), impact-crater depth (d), central-peak diameter (D_{cp}), height of central peak (h_{cp}) and height of impact crater rims (H). Except for the central peak diameter all of the obtained values are far out of range suggesting a non-impact origin for the depression.

more amounts of volatiles when compared to the main debris apron. Deformation at the zone of coalescence would also imply ongoing advance of the main debris apron during formation of the debris tongue. To explain this scenario, there must have been a more or less sudden release of volatiles and debris which was triggered by an unknown event leading to formation of the debris tongue at a time when advance of debris aprons was still an ongoing process. Release of volatiles from the apron would have been be necessary as the formation of such a tongue-shaped morphology (length/width≫7) requires significantly lower yield stresses than the lobate landforms (length/width≤1).

Topographically, there are no indications which could have supported a confined and therefore significantly elongated flow explaining the characteristic shape of

the debris tongue. However, we cannot observe indications on the debris apron which allow us to draw such a conclusion. Major release of material (volatiles as well as debris) would imply a remarkable subsidence of the main debris apron surface. Still it cannot be completely excluded as ongoing debris-apron advance could have filled any morphological signs that were caused by material removal similar to the first scenario.

[3] A third scenario consists of formation of the debris tongue considerably later than emplacement of the debris apron. A similar scenario has been suggested by *Baratoux et al.* (2002) because of the minor amount of impact craters observed on the debris tongue. Although we can confirm this observation by own dating efforts with which the crater-size frequency distribution would yield an model age of 5-15 Ma for the

debris tongue and 45 Ma for the debris-apron lobe according to martian crater scaling laws (*Soderblom et al.*, 1974; *Neukum and Wise*, 1976; *Neukum and Hiller*, 1981; *Stöffler and Ryder*, 2001; *Hartmann*, 1977; *Ivanov*, 2001; *Neukum et al.*, 2001) and the impact cratering model of *Hartmann and Neukum* (2001) with polynomial coefficients by *Ivanov* (2001), it is still an open question, why debris apron material is superimposed on the debris tongue if the last active resurfacing phase is much older than that of the debris tongue. Ages of the debris apron lobe can be considered as upper limit, results are comparable to measurements performed by *Head et al.* (2005) for a debris apron farther to the north. Nevertheless, crater counting on landforms where concentric depressions and circular hollows are an important indicator of the morphologic inventory are questionable. We exclude this scenario due to the same reasons as for the similar second scenario.

The derivation of a relative sequence of events and the determination of meaningful absolute ages require a clear understanding and thorough mapping of material and geologic units. Based on the complexity of this terrain it is quite complicated to distinguish between different units and therefore determination of absolute ages are not possible. Furthermore, although geomorphologically the landslide units observed her are different, lithologically they are identical.

The state of degradation of the volcanic caldera suggests a rather old age which might be roughly consistent with the time of formation of the Harmakhis Vallis outflow channel. Later activity - either volcanic, seismic or erosional - caused collapse of the depression rims and (a) partly infill of Harmakhis Vallis, (b) formation of various landslide units through rim collapse and formation of the discussed debris tongue. Decoupled from any volcanic processes, volatile content inside of landslide units caused ongoing deformation and creep which lasted until more recent times. Deformation processes caused movement of the entire debris body, differential advance of discrete units is not observed.

The timespan between debris-tongue formation and debris apron advance cannot be estimated correctly

nor can the absolute age be derived, as statistics based upon crater-size frequency distributions are misleading at this very configuration.

When inspecting the debris apron surface not only arcuate troughs and bended depressions can be observed but also a plethora of circular or slightly elliptical depressions. Almost all of these features are prone to be interpreted as impact craters that are either relatively fresh or slightly deformed. When interpreting landforms with considerable volatile contents, degradational morphologies such as thermokarst depressions which form circular to elliptical depressions have to be taken into account. In conclusion, crater measurements such as performed by *Baratoux et al.* (2002) have to be interpreted with much care. Resurfacing ages for both units, debris tongue and debris apron, are presumably similar, the landforms however are probably much older and suffered from intense degradation and surface disintegration.

9.5. Summary and Conclusions

Examinations of the debris-tongue feature as well as the broader geomorphologic context of the Hellas Montes area have shown that a landslide or avalanche origin as proposed by (*Baratoux et al.*, 2002) for this spatulate landform is generally conceivable. At large scale, its general spatulate shape and well-pronounced margins are roughly comparable to terrestrial debris-avalanche landforms.

More detailed analyses of its morphology and its textural properties on the basis of HRSC, THEMIS and high-resolution MOC data gave more insights into the development and deformation history of the spatulate landform and provided observational evidence for a transitions of high-energy rapid emplacement to long-lasting creep deformation. Except for the general shape, surface characteristics and microrelief are more akin to landforms indicative of slow creep and deformation known and observed at abutting lobate debris aprons as well. These characteristics comprise margin-parallel arcuate ridges and furrows that are mostly intact and indicate undisturbed advance of coherent masses of debris. Marginal lobes
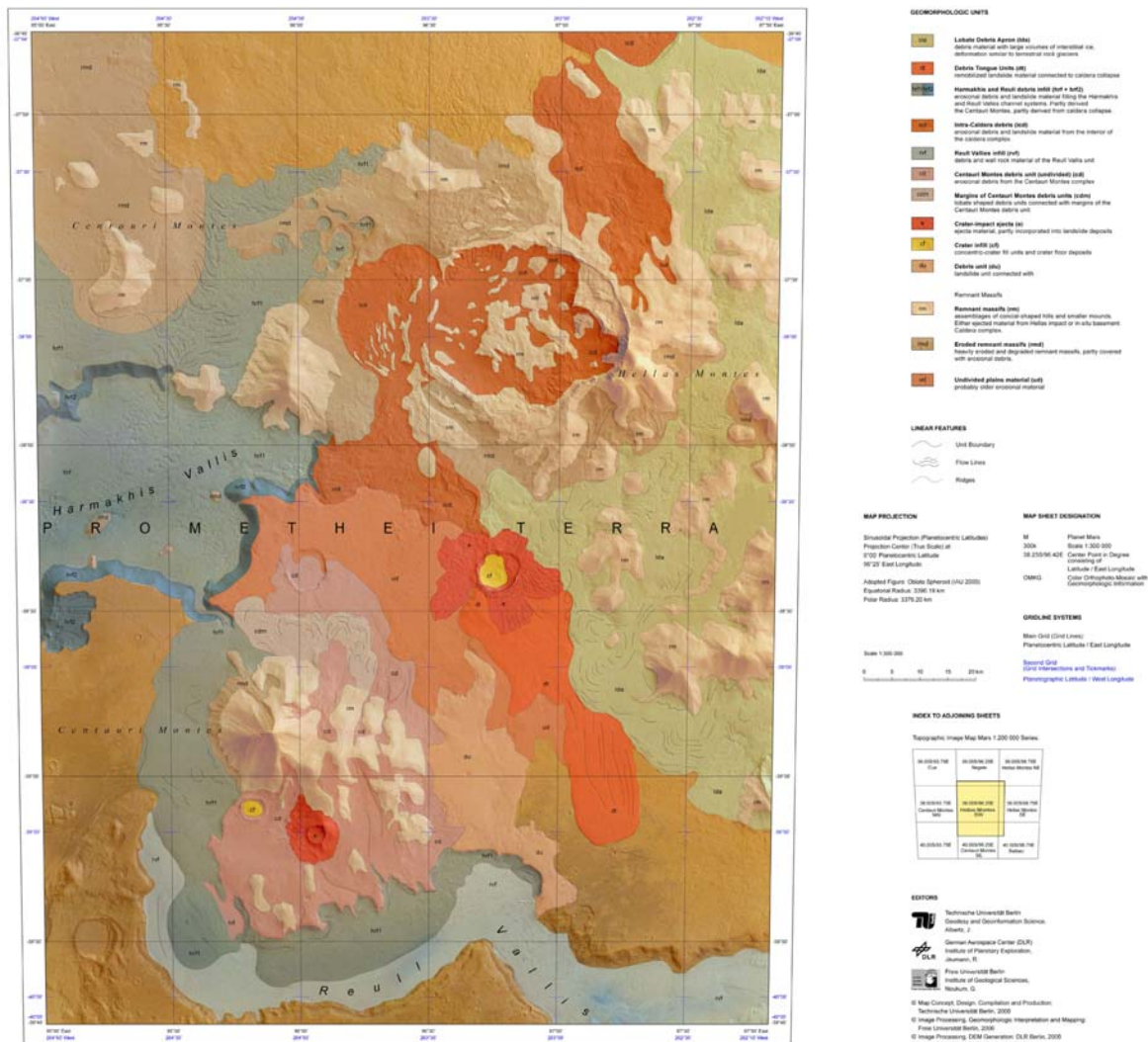
Figure 9.15.: Geomorphic map of the Hellas Montes/Centauri Montes region, 1:300,000 (38.25S/96.42E OMKG), HRSC team co-operation between Freie Universität Berlin (FUB) and Technical University of Berlin (TUB), mapping by S. van Gasselt (FUB), map layout and cartography by H. Lehmann and S. Gehrke (TUB), see also *Lehmann et al.* (2006b,a) (note, figure is not included in the original manuscript currently in press in J. Geophys. Res. (*van Gasselt et al.*, 2007)).

frequently observed with avalanches and indicative of water-rich slurries are missing indicating a considerable internal strength typical of rock glacier-like flow. Wave propagation hummocks or accumulation of boulders common on high-energetic terrestrial avalanches (*Brantley and Glicken*, 1986; *Crandell*, 1989; *Glicken*, 1996) are missing. Complex coalescence morphologies at transitions between the spatulate landform and adjacent debris units indicate comparable rheologies. Contrasting to earlier assumptions by *Baratoux et al.* (2002), MOLA-based topographic data reveal a convex-shaped terminus similar to the shape of termini of lobate debris aprons that have been interpreted as results of the deformation

of glacial (*Paterson*, 2000; *Hooke*, 2005) or ice-rich debris systems (*Wahrhaftig and Cox*, 1959; *Barsch*, 1988, 1996; *Whalley*, 1992) on the Earth and on Mars (*Squyres*, 1978, 1979). The proposed concave profile seen by *Baratoux et al.* (2002) is restricted to the intermediate zone of the debris tongue only and is caused by degradation of the spatulate landform. Comparable concave profiles have often be attributed to a degraded and fossil state of terrestrial rock glaciers (e.g., *Ikeda and Matsuoka*, 2002; *Berthling et al.*, 1998). Beside the concave shape, small-scaled surface features also indicate traces of degradation after emplacement: circular to elliptical pits and cavities compare closely to karst-degradation morphologies as known from thermokarst in periglacial environments (*French*, 1996) or glacial karst within glacial systems (*Menzies*, 2002; *Benn and Evans*, 2003). Other sets of degradational morphologies comprise fretted and dissected mantling deposits at the eastern and frontal margins and traces of disintegration of the uppermost surface layer of the debris tongue. The fossil state of the rock glacier landform is also consistent with modelling work performed by *Colaprete and Jakosky* (1998) that suggests that nowadays temperatures are too low to aid rock glacier formation. We consider a genetic classification of that particular landform based on morphometry only as conducted by *Baratoux et al.* (2002) as too speculative. Terrestrial derived morphometric values for various debris-water transport systems are not directly comparable to Martian systems because of different environmental influences and uncertain formation conditions which result in imponderabilities. Even in terrestrial environments there has been considerable confusion about classifications of various types of debris-water transport systems *Iverson* (1997) and even the microrelief of genetically similar landforms can differ significantly depending on the thermal regime in which they exist (*Kääb et al.*, 2002).

We have found observational evidence that the debris tongue has a landslide origin connected to a 35-km-diameter depression in the north that was interpreted as impact-crater structure. Morphometric comparisons with global datasets by *Garvin et al.* (1999, 2000a,b) give reasons to believe that an impact origin is less likely. Large-scale wall-rock failures and abundant evidence for massive mass-wasting at the interior and the surroundings of the depression suggest a large collapse of a caldera complex during which the debris tongue was formed initially (figure 9.12). Future work has to show in how far a volcanic construct might have contributed to the formation of Harmakhis Vallis and in how far explosive volcanism contributed to supply of material for debris apron formation.

The degradational characteristics suggest that the landslide has undergone post-emplacement modifications transferring the landslide into a ice-debris mixture which deformed slowly comparable to rock glaciers on the Earth. Such processes are reasonably known and caused lots of confusion even at places that are much better accessible through field investigations (*Johnson*, 1974, 1984; *Whalley*, 1976; *Vick*, 1981; *Whalley*, 1992; *Whalley and Azizi*, 2003).

Absolute and relative age determinations are limited here due to the complexity of surface textures as well as similarities of morphologies of impact craters and degradation pits. Although the origin of the landslide might date back to hundreds of million years ago, later debris-movement caused resurfacing during cold-climate epochs which caused obliteration of impact craters and masking of true ages.